



OPEN ACCESS

EDITED BY

Giorgio Treglia,
Ente Ospedaliero Cantonale (EOC), Switzerland

REVIEWED BY

Angelo Castello,
IRCCS Ca' Granda Foundation Maggiore
Policlinico Hospital, Italy
Carmelo Caldarella,
Fondazione Policlinico Universitario A. Gemelli
IRCCS, Italy
Salvatore Annunziata,
Fondazione Policlinico Universitario A. Gemelli
IRCCS, Italy

*CORRESPONDENCE

Cristina Nanni
✉ cristina.nanni@aosp.bo.it

[†]These authors have contributed equally to this work

RECEIVED 12 April 2023

ACCEPTED 19 May 2023

PUBLISHED 06 July 2023

CITATION

Nanni C, Mosconi C, Dragonetti V, Barakat M, Fraccascia N, Coccozza MA, Brocchi S, Palloni A, Paccapelo A, Brandi G and Fanti S (2023) Prognostic value of integrated morphofunctional imaging methods in inoperable intrahepatic cholangiocarcinoma. *Front. Med.* 10:1204717. doi: 10.3389/fmed.2023.1204717

COPYRIGHT

© 2023 Nanni, Mosconi, Dragonetti, Barakat, Fraccascia, Coccozza, Brocchi, Palloni, Paccapelo, Brandi and Fanti. This is an open-access article distributed under the terms of the [Creative Commons Attribution License \(CC BY\)](https://creativecommons.org/licenses/by/4.0/). The use, distribution or reproduction in other forums is permitted, provided the original author(s) and the copyright owner(s) are credited and that the original publication in this journal is cited, in accordance with accepted academic practice. No use, distribution or reproduction is permitted which does not comply with these terms.

Prognostic value of integrated morphofunctional imaging methods in inoperable intrahepatic cholangiocarcinoma

Cristina Nanni^{1*†}, Cristina Mosconi^{2†}, Valentino Dragonetti³, Massimo Barakat², Nicola Fraccascia³, Maria Adriana Coccozza², Stefano Brocchi², Andrea Palloni⁴, Alexandro Paccapelo², Giovanni Brandi^{4,5} and Stefano Fanti^{1,2,3}

¹Nuclear Medicine Unit, IRCCS Azienda Ospedaliero-Universitaria di Bologna, Bologna, Italy, ²Radiology Unit, IRCCS Azienda Ospedaliero-Universitaria di Bologna, Bologna, Italy, ³Nuclear Medicine, Alma Mater Studiorum, University of Bologna, Bologna, Italy, ⁴Medical Oncology, IRCCS Azienda Ospedaliero-Universitaria di Bologna, Bologna, Italy, ⁵Department of Internal Medicine and Surgery, Alma Mater Studiorum, University of Bologna, Bologna, Italy

Introduction and aim: Intrahepatic cholangiocarcinoma (iCCA) is a disease characterized by rarity, heterogeneity, and high mortality, where surgical resection is often not possible. Nowadays, due to the recent introduction of new therapeutic options such as trans-arterial radioembolization (TARE), it is increasingly important to define the role of morphofunctional imaging methods for the prognostic stratification of patients affected by iCCA. The aim of the study was to verify the prognostic value of morphofunctional imaging methods at the baseline in patients with inoperable iCCA.

Methods: In total, 45 patients with iCCA were sent to our center between January 2016 and March 2021 for being evaluated to be treated with TARE. All of them underwent both [18F]-FDG-PET/CT and contrast-enhanced CT (ceCT) in a single procedure and were included in our study. The inclusion criteria were as follows: a diagnosis of inoperable iCCA; both [18F]-FDG-PET/CT and ceCT scans; and washout from therapy for at least 2 months before baseline [18F]-FDG-PET/CT and ceCT scans. Both clinical and laboratory data and baseline imaging data (ceCT and [18F]-FDG-PET/CT) were collected. In particular, regarding clinical and laboratory data, we collected overall survival (OS), gender, age, prior therapies, liver function indices, and tumor markers. Regarding ceCT, we collected TNM staging, lesion diameter, volume, vascularization, and presence of intravascular necrosis. Regarding [18F]-FDG-PET/CT, we collected TNM staging, Standard-Uptake-Value max (SUVmax), Metabolic-Tumor-Volume (MTV), and Total-Lesion-Glycolysis (TLG=MTV*lesions SUVmean). Philips-Vue-PACS software was used, setting hepatic SUVmean as TLG threshold.

Results: A statistically significant correlation was found between some examined parameters at morphofunctional investigations at the baseline and OS. [18F]-FDG-PET/CT parameters statistically correlated with OS were the stage of disease greater than M0 ($p = 0.037$), major lesion SUVmax ($p = 0.010$), MTV ($p \leq 0.001$), and TLG ($p < 0.001$). Other parameters at ceCT correlated with OS were the stage of disease greater than T2 ($p = 0.038$), maximum lesion diameter ($p = 0.07$), volume of the major lesion ($p = 0.016$), and total volume of lesions ($p = 0.009$). Biochemical parameters correlated with OS were gamma glutamyl transferase (GGT, $p = 0.014$), alkaline phosphatase (ALP, $p = 0.019$), carcinoembryonic antigen (CEA, $p = 0.004$), and carbohydrate antigen 19-9 (CA 19-9, $p < 0.001$). From the parameters estimated by the multivariate model, we derived a four-variable score for OS combining nodal involvement and SUVmax at [18F]-FDG-PET/CT, GGT, and CA 19-9 levels.

Conclusion: Considering our data, performing integrated pre-therapy imaging is critical for the prognostic stratification of patients with iCCA.

KEYWORDS

intra-hepatic cholangiocarcinoma, FDG PET/CT, ceCT, prognostic value, TARE

1. Introduction

Cholangiocarcinoma (CCA) is the most common biliary malignancy and the second most common hepatic malignancy after hepatocarcinoma (1, 2), with more than 95% of CCA are ductal adenocarcinomas that arise from the epithelium of the biliary tract (3). Several risk factors, such as parasitic infections, toxins, hepatitis B and C, and primary sclerosis cholangitis (PSC) are correlated with the risk of developing CCA (3).

CCA are divided into three types, according to their anatomical localization, such as intrahepatic cholangiocarcinoma (iCCA), perihilar cholangiocarcinoma (pCCA, also known as Klatskin tumor), and extrahepatic cholangiocarcinoma (4). iCCA is the least common variant of CCA, representing 10–20% of all CCA diagnosed, but several studies globally reported increased rates of iCCA in the last few decades (5–8). Given the prevalence of paucisymptomatic clinical figures and the lack of any screening programs, up to 70% of patients are diagnosed with locally advanced or metastatic disease, precluding surgical intervention, which nowadays represents the only available treatment (9, 10), and, outside curative option, iCCA has a high mortality rate, with only 5–10% of patients with unresectable disease alive 5 years after initial diagnosis (3), with the combination of gemcitabine/cisplatin chemotherapy and immunotherapy, considered as the new first-line treatment option.

Given the current treatment limitations, there is a need for the implementation of new therapy options, such as TACE and TARE, that nowadays are commonly used only for palliative purposes. To do so, it is important to evaluate the role of multimodality imaging, considering its importance not only for diagnosis and staging but also for the correct management of patients with iCCA.

Among the main imaging methods for iCCA, there is ceCT, which is mainly used for diagnosis and staging, with reported sensitivity and specificity values in the literature of nearly 78 and 80%, respectively (11, 12). In particular, it is characterized by the detection of lesions with irregular margins with early peripheral enhancement and late central enhancement. Different studies have shown how ceCT can better assess tumor infiltration of perilesional vascular structures (13), as well as a high capacity to define the resectability of such lesions, with a negative predictive value of 85–100% (14). The diagnostic accuracy of ceCT in the evaluation of lymph node involvement is approximately 77% (15). ceCT can also diagnose distant metastases, frequently involving the peritoneum, lungs, and bone (16).

Another imaging method used in the diagnosis of iCCA is magnetic resonance imaging (MRI), with sensitivity and specificity

for small lesions reported in the literature of nearly 77 and 96%, respectively (17).

[18F]-FDG-PET/CT is currently used mainly in the detection of distant metastases, rather than for primary lesions assessment, with a recent meta-analysis showing a sensitivity and specificity of 95 and 93%, respectively (18), which is higher than ceCT for this indication (19, 20).

Some authors demonstrated how some semi-quantitative parameters of [18F]-FDG-PET/CT, such as SUVmax, may be related to the risk of recurrence and OS (21), as well as how additional parameters such as MTV and TLG are predictive of 5-year survival rates (22).

Given this, the aim of our study was to evaluate the impact of baseline [18F]-FDG-PET/CT in the prognostic stratification of patients with inoperable iCCA who reached our center for being evaluated for TARE.

2. Materials and methods

The study conforms to the ethics guidelines of the Declaration of Helsinki, and data collection and analyses had already previously been approved by our Institutional Review Board and ethical committee of S. Orsola Hospital (193/2021/Oss/AOUBo). All patients provided informed written consent for the TARE and for the processing of personal data according to the Italian Data Protection Authority law (legislative decree n. 196 of 2003 and n. 101 of 2018).

A total of 45 patients were sent to our center by other centers for being evaluated for an eventual TARE between January 2016 and March 2021. All of them had a diagnosis of inoperable iCCA and were out of therapies for at least 2 months. All the enrolled patients underwent a combined imaging procedure including a [18F]-FDG-PET/CT and ceCT (GE, Discovery MI DR or GE, Discovery D710 equipped with a 64 slices CT). Patients for whom TARE was not indicated underwent different systemic treatments.

Patients were eligible for this treatment if they met the following criteria: (1) histologically proven ICC; (2) unresectable naive tumor or disease relapse/persistence after various treatments, including liver resection; (3) Eastern Cooperation Oncology Group (ECOG) performance status of 0–2; (4) adequate liver function with bilirubin <2.0 mg/dL; (5) granulocyte count $\geq 1.5 \times 10^9/L$; (6) platelet count $\geq 50 \times 10^9/L$, and (7) amenability to visceral angiography. The exclusion criteria included (1) flow to the gastrointestinal tract not correctable by coil embolization or (2) estimated lung exposition to a radiation dose >30 Gray (Gy).

2.1. [18F]-FDG-PET/CT images

[18F]-FDG-PET/CT scans were performed as per the standard procedure suggested by EANM guidelines (23).

Briefly, patients were not allowed to consume any food or sugar for at least 6 h prior to the start of the [18F]-FDG-PET/CT study. The injected dose was 2–3 MBq/Kg. The uptake time was 60 ± 10 min. Pain medications were allowed but corticosteroids were forbidden. The field of view must include the skull up to the mid-thigh. Acquisition time was 2 min/bed position. Low-dose CT was acquired at 120 kV and 80 mA. Iterative reconstruction (3D ordered subsets expectation maximization with 2 iterations, 20 subsets, followed by smoothing with a 6-mm 3D Gaussian kernel) and CT-based attenuation, scatter, random coincidence events, and system dead-time iterative correction of emission data can be applied to obtain high-quality PET images (24).

2.2. Computed tomography images

ceCT was performed immediately after the PET study. A solution of 71.44% w/v of iomeprol equivalent to 35% iodine or 350 mg iodine/ml (Iomeron 350) was used as IV contrast media and was administrated in a dosage corresponding to 100–150 ml depending on patient weight.

All the patients underwent a multiphase-modulated CT with the following scheme:

1. thorax, abdomen, and pelvis without i.v. contrast agent
2. superior abdomen in an early arterial phase
3. superior abdomen in a late arterial phase
4. thorax, abdomen, and pelvis in a venous phase
5. abdomen and pelvis in a late phase at 4 min since the contrast media injection.

After infusion of the contrast agent at a rate of 3–4 mL/s, the early hepatic arterial phase was determined using a region of interest (ROI) placement in the abdominal aorta at the level of the celiac artery, and the CT scan was initiated when achieving a peak of at least 150 Hounsfield units (HU) within the ROI; the late arterial phase, venous phase (70–80 s), and a late phase (4 min) were then acquired.

CT images were reconstructed as follows:

- HRCT on the thorax with a lung filter
- soft tissue filter and 2.5 mm slice thickness for the other series.

The volume analysis was performed using Philips IntelliSpace portal[®]. The evaluation of intrahepatic vascular and biliary anatomy is fundamental to obtain an accurate liver volume estimation. An expert radiologist (more than 10 years of experience) manually traced the contour of the major lesion and the contour of the total volume of disease, on every slice of portal venous phase CT. Subsequently, the software provides to calculate the volume of the region of interest segmented (Figure 1).

TARE procedure: When indicated, radioembolization therapy was carried out according to a technique previously described in detail elsewhere (25, 26).

Chemotherapy treatment: Patients with residual or intra/extrahepatic progressive disease were treated with systemic chemotherapy according to age, performance status, and liver function. The combination of cisplatin and gemcitabine was the preferred first-line treatment option in patients with good performance status (ECOG PS 0-1) and preserved liver function, while gemcitabine monotherapy was administered in unfit and/or elderly patients.

2.3. Staging and follow-up

ceCT data considered were TNM staging, lesion vascularization, presence of intralesional necrosis, maximum lesion transversal diameter (expressed in millimeters), major lesion volume, and total volume of disease (both expressed in square centimeters).

[18F]-FDG-PET/CT parameters evaluated were TNM staging, SUVmax, MTV, and TLG. In order to collect semi-quantitative data, all [18F]-FDG-PET/CT scans were retrospectively re-evaluated, using Philips-Vue-PACS software and setting hepatic SUVmean as TLG threshold.

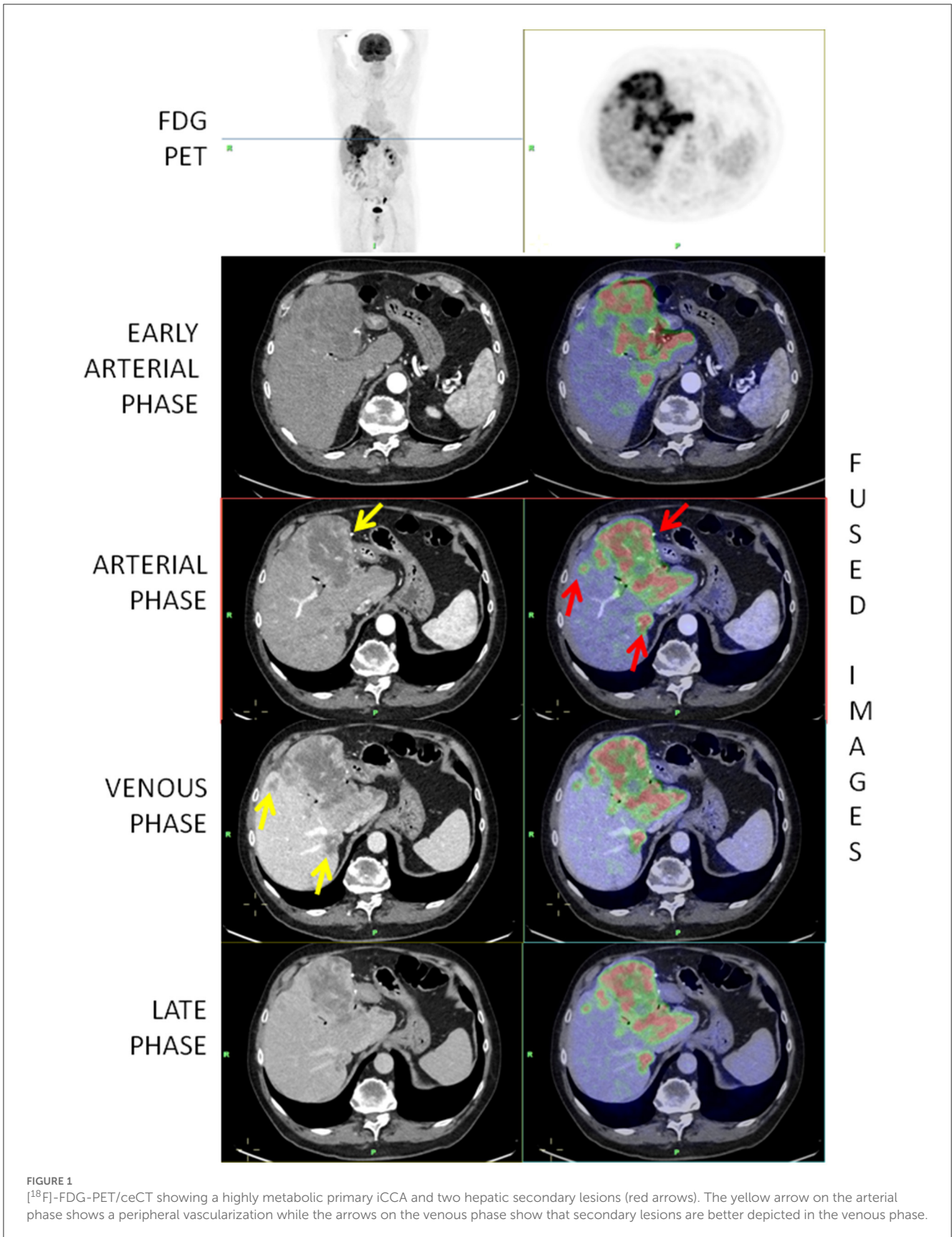
After treatment, the patients were regularly evaluated at 1 and 3 months, and thereafter at 3-month intervals. At each visit, clinical data were recorded, and CT or magnetic resonance imaging (MRI) was performed. The following blood tests data were also collected: aspartate aminotransferase (AST), alanine transaminase (ALT), GGT, ALP, total bilirubin, CEA, CA 19-9, and alpha fetoprotein (AFP). All clinical, laboratory, and imaging data were prospectively collected.

OS data, with a median follow-up of 47.9 months, were also evaluated and correlated with the above-mentioned variables.

2.4. Statistical analysis

Data were reported as mean \pm standard deviation or frequencies. The Kolmogorov–Smirnov test with Lilliefors correction was used to assess the distributional normality of the variables. Survival data were estimated and represented graphically by the Kaplan–Meier method. For survival analyses, hazard ratios with their 95% confidence intervals were estimated by univariate and multivariate Cox regression models. The forward stepwise choice procedure based on the likelihood ratio with an input *p*-value of 0.050 and an output *p*-value of 0.100 was used to choose variables in the multivariate models. A score was calculated with parameters estimated from the multivariate model. Best cutoffs were estimated by maximizing the Youden index and evaluating any local maxima for OS at 12 months. Two-tailed tests with a *p*-value of <0.05 were considered to be statistically significant. All analyses were performed with IBM SPSS 27.0 software (SPSS Inc., Armonk, NY, USA).

From the parameters estimated by the multivariate analysis, we derived a score for OS combining [18F]-FDG-PET/CT, ceCT, and clinical data. The score was therefore calculated according to the following formula: $N\text{-PET-stage} * 1.834 + \log_{10}(\text{GGT}(\text{UL})) * 0.969 + \log_{10}(\text{CA 19-9}(\text{Uml})) * 0.714 + \text{SUVmax} * 0.087$. We found two



local maxima correlated to OS at 12 months, so we grouped the score into three categories considering group 1 for results <3.5, group 2 between 3.5 and 4.7, and group 3 for values >4.73.

3. Results

3.1. Patient characteristics

Of the 45 patients enrolled, 25 were men (55.6%) and 20 were women (44.4%), with an average age of 62.9 years (range 29–86y). A total of 31 patients (68.9%) had undergone prior therapies: 11 surgery, 6 local therapies, and 14 chemoembolization.

Information regarding therapy following multidisciplinary imaging methods was available for 21 patients, of whom the indication for TARE was confirmed in 38% of cases, while the others were referred to other systemic treatment approaches.

At ceCT, five patients were categorized as T1 (11.1%), 19 as T2 (42.2%) and 21 as T3 (46.7%); 24 as N0 (53.3%) and 21 as N1 (46.7%); 20 as M0 (44.4%) and 25 as M1 (55.6%).

In the vast majority of cases, the vascularization of the lesions was peripheral (43; 95.6%) (Figure 1), whereas in only one case, the lesions were hypodense and in one case, it was hyperdense. Intralesional necrosis was present in 35 cases (77.8%) and absent in 10 (22.2%).

The mean maximum transverse diameter of the largest lesion was 76.2 mm. The mean of the largest lesion volume was 321.7 cm³, and the mean of the total lesion volume was 414.9 cm³.

At [18F]-FDG-PET/CT, two patients showed no hypermetabolic primary lesion and were therefore categorized as T0 (4.4%), 13 as T1 (28.9%), 19 as T2 (42.2%), and 11 as T3 (24.4%); 41 as N0 (91.9%) and 4 as N1 (8.9%); 24 as M0 (53.3%), and 21 as M1 (46.7%).

The mean SUVmax was 12.8. The mean MTV was 479.0 cm³, with a mean TLG of 2742.2.

The population characteristics are summarized in Table 1.

3.2. Determinants of survival

According to the univariate analysis, the parameters correlated with OS in a statistically significant way were as follows: at ceCT, T3 stage (HR = 3.725; $p = 0.038$), maximum transaxial lesion diameter (HR = 1.013; $p = 0.007$), major lesion volume (HR = 2.023; $p = 0.016$) and total volume disease (HR = 2.261; $p = 0.009$); at [18F]-FDG-PET/CT, presence of distant metastases (HR = 1.982; $p = 0.037$), SUVmax (HR = 1.050; $p = 0.010$), MTV (HR = 4.256; $p < 0.001$), and TLG (HR = 3.433; $p < 0.001$); at biochemical analysis, GGT (HR = 2.621; $p = 0.014$), ALP (HR = 4.679; $p = 0.019$), CEA (HR = 2.781; $p = 0.004$), and CA 19-9 (HR = 2.923; $p < 0.001$).

Moreover, the following parameters did not correlate with OS in a statistically significant manner: at ceCT, stage \leq T2, stage N and M; at [18F]-FDG-PET/CT, stage T and N; gender, prior therapies, presence of intralesional necrosis, AST, ALT, total bilirubin, and AFP.

On multivariate analysis, the presence of lymph node metastases at PET scan (HR = 6.261; $p = 0.090$), SUVmax (HR

= 1.091; $p < 0.001$), GGT (HR = 2.634; $p = 0.031$), and CA 19-9 (HR = 2.043; $p = 0.012$) were found to be independent prognostic factors for OS (Figure 2).

Regarding the survival curve of N1 patients, it must be noted that it is much steeper than that for the N0 stage in the first 5–10 months, and then it is flat. This is because the clinical conditions of three patients worsened rapidly while one is still alive after more than 4 years. One patient behaved totally differently from the other 3. This heavily impacts on the statistical analysis and explains why the p -value ($p = 0.09$) is the highest among the four parameters selected by the multivariate analysis, next to the limit of acceptability.

Dividing the patient population according to the pre-enrolling care, these parameters did not reach a statistically significant level ($P = 0.149$). Furthermore, pre-enrollment care appears to be unrelated to N-positive/negative lymph nodes ($P = 1.000$) nor superior/inferior SUVmax of lesions ($P = 0.132$).

The aforementioned derived score of OS combines PET, CT, and clinical data. It showed to be correlated to OS in a statistically significant way: for patients with a score of 1, mOS = 48.1; for a score of 2, mOS = 13.7 (HR: 15.9; $p = 0.009$); for a score of 3, mOS = 3.0 (HR: 53.8; $p < 0.001$) (Figure 3).

The results derived from the score were confirmed after splitting the population in treated patients (overall log-rank test for OS: $P < 0.001$), and naive patients (overall log-rank test for OS: $P = 0.016$).

4. Discussion

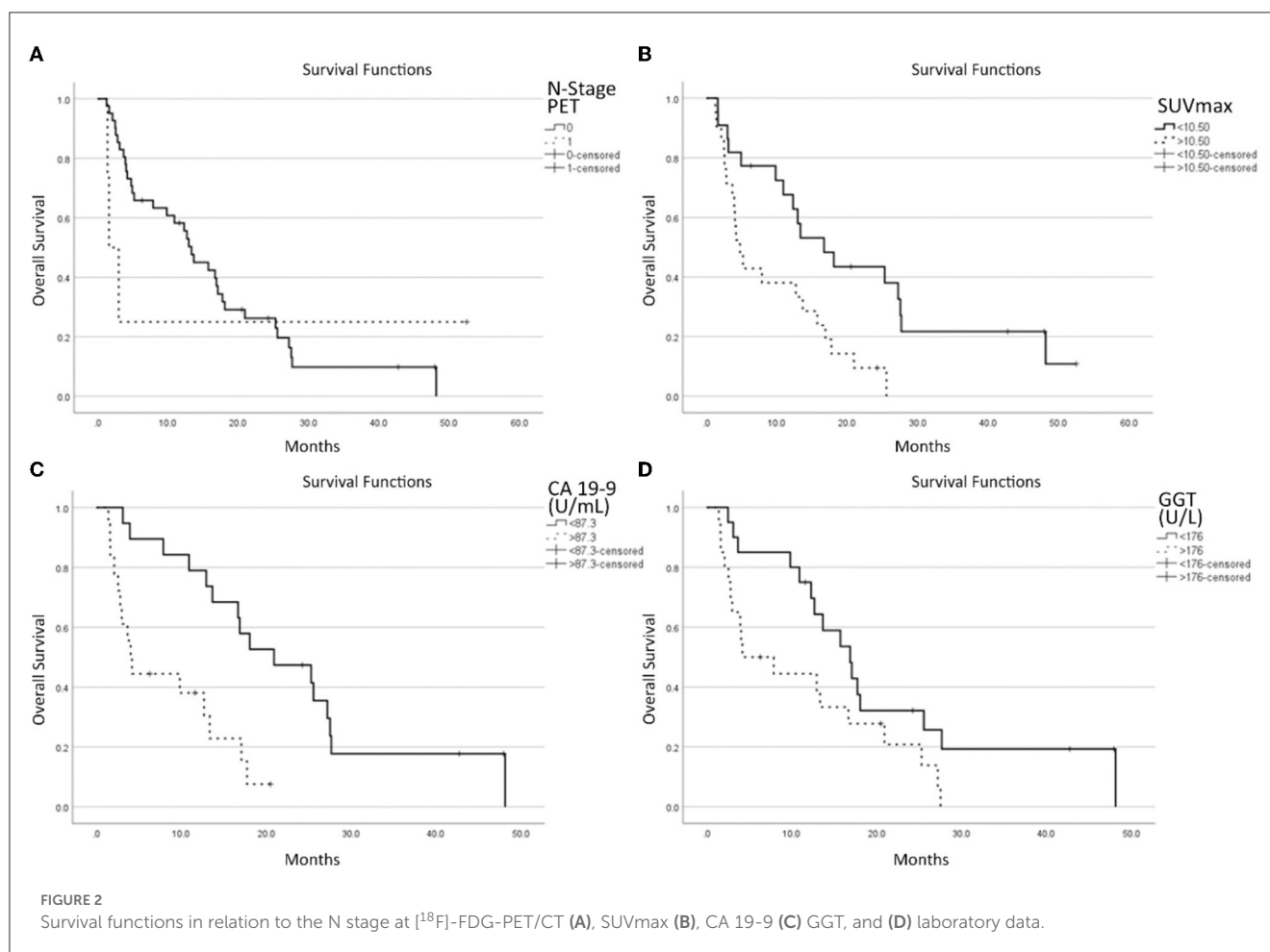
According to the latest National Comprehensive Cancer Network (NCCN) guidelines, the imaging evaluation of iCCA should include hepatic lesion extension, lymph node, and distant metastases, considering that metastatic lymph nodes over the hepatic hilum and hepatic metastases should be considered as distant metastases, preventing from curative surgery (27).

The ceCT offers a high prognostic value in terms of survival and the vascularization and the diameter embody the main biomarkers for this assessment. Actually, it is widely well-known in the scientific literature that enhancement patterns correlate with tumor spread and survival (28–30). The ICC patterns are hypovascular, rim-like, and hypervascular. The first one shows the highest frequency of lymphatic, perineural, and biliary dissemination, and a low survival rate at 1 and 3 years, with 30.7 and 0%, respectively. On the contrary, the hypervascular ICC pattern displays lower rates of invasion and the longest survival at 1 and 3 years, with 88.9 and 66.7%, respectively (27). However, in our study, the largest part of patients presented a rim-like pattern, and consequently, this parameter did not affect the prognostic score proposed. Moreover, the diameter depicts the second key factor that should be taken into account for a prognostic evaluation of ceCT in patients affected by ICC. As shown in literature, the diameter represents a crucial factor in radiomics studies which allows to predict both patients with low risk of early intrahepatic recurrence and the response to target therapies, such as TARE (31, 32). Indeed, in accordance with the literature, in our study, the diameter is confirmed as a parameter statistically significant according to the univariate analysis and therefore correlated with survival.

TABLE 1 Population characteristics, in particular gender, previous therapies, lesion characteristics such as vascularization and necrosis, data collected from ceCT, [¹⁸F]-FDG-PET/CT, and laboratory data.

		n	%	mOS	Univariate				Multivariate			
					HR	CI 95%	p	HR	CI 95%	p		
Patients		45	100.0									
Gender	F	20	44.4	13.7	ref							
	M	25	55.6	9.8	1.276	0.672	2.423	0.457				
Prior Therapies	No Therapy	14	31.1	12.7	ref							
	Chemotherapy	14	31.1	4.2	1.151	0.493	2.684	0.745				
	Surgery	11	24.4	16.9	1.013	0.437	2.350	0.975				
	Loco-regional	6	13.3	13.3	0.657	0.224	1.930	0.445				
Vascularization	Peripheral	43	95.6									
	Ipodense	1	2.2									
	Hyperdense	1	2.2									
Necrosis	Absent	10	22.2	18.1	ref							
	Present	35	77.8	10.9	1.986	0.900	4.382	0.890				
CECT	T1	5	11.1	27.2	ref							
	T2	19	42.2	12.7	2.683	0.767	9.381	0.122				
	T3	21	46.7	7.9	3.725	1.077	12.889	0.038				
	N0	24	53.3	13.7	ref							
	N1	21	46.7	9.8	1.443	0.757	2.749	0.265				
	M0	20	44.4	13.7	ref							
	M1	25	55.6	12.3	1.726	0.891	3.343	0.106				
[¹⁸ F]-FDG-PET/CT	T0	2	4.4	17.1	0.883	0.110	7.084	0.907				
	T1	13	28.9	15.7	ref							
	T2	19	42.2	13.3	1.453	0.644	3.278	0.368				
	T3	11	24.4	4.8	2.419	0.991	5.908	0.052				
	N0	41	91.1	13.3	ref							
	N1	4	8.9	1.6	1.048	0.304	3.611	0.941	6.261	0.752	52.144	0.090
	M0	24	53.3	16.7	ref							
	M1	21	46.7	4.9	1.982	1.041	3.776	0.037				
	Mean			SD								
Age (y)		62.9	±	13.2	0.993	1.041	3.776	0.506				
CECT	max Ø (mm)	76.2	±	38.1	1.013	1.004	1.023	0.007				
	> Lesion Vol (cm³)	321.7	±	408.6	2.023	1.138	3.595	0.016				
	Tot Lesion Vol (cm³)	414.9	±	577.2	2.261	1.225	4.173	0.009				
[¹⁸ F]-FDG-PET/CT	SUVmax	12.8	±	8.2	1.050	1.012	1.091	0.010	1.091	1.040	1.114	<0.001
	MTV	479.0	±	667.1	4.256	2.132	8.497	<0.001				
	TLG	2,742.2	±	4,179.7	3.433	1.900	6.205	<0.001				
Lab Data	AST (U/L)	57.7	±	44.9	1.610	0.382	6.783	0.516				
	ALT (U/L)	53.7	±	64.0	0.972	0.323	2.921	0.960				
	GGT (U/L)	360.7	±	420.1	2.621	1.217	5.645	0.014	2.634	1.094	6.344	0.031
	ALP (U/L)	253.8	±	187.8	4.679	1.290	16.967	0.019				
	Tot Bilirubin (mg/dL)	1.5	±	2.0	2.170	0.652	7.225	0.207				
	CEA (ng/mL)	8.8	±	22.2	2.781	1.391	5.557	0.004				
	CA 19-9 (U/mL)	815.2	±	2,697.0	2.923	1.717	4.979	<0.001	2.043	1.173	3.558	0.012
AFP (ng/mL)	40.7	±	126.2	1.000	0.995	1.004	0.811					

Mean OS follow-up: 47.9 months. n, number of patients; %, percentage of patients; mOS, months of overall survival; HR, hazard ratio; CI95%, confidence interval 95% p, probability index; N1, positive lymphnode; M1, positive metastasis; max Ø (mm), maximum diameter in mm; Mean, mean value; SD, standard deviation; > lesion Vol (cm³), volume in cm³ of the biggest lesion; Tot lesion vol (cm³), total volume of all the lesions in cm³; SUV mxs maximum, standardized uptake value; MTV, metabolic tumor volume; TLG, total lesion glycolysis; GGT, Gamma-glutamyl Transferase; ALP, Alkaline Phosphatase; CEA, carcinoembryonic antigen; CA 19-9, Carbohydrate antigen 19-9. In bold are the values with the lowest Pearson correlation coefficient, with the corresponding name also bolded.



Regarding $[^{18}\text{F}]$ -FDG-PET/CT, many studies in the literature have already highlighted its crucial role in the oncological management of patients with cholangiocarcinoma at the diagnostic stage (11, 33–35), as well as a statistical correlation between semi-quantitative parameters such as SUVmax, MTV, and TLG with OS (21, 22).

In our study, we have demonstrated that the combination of FDG PET/CT, multiphase ceCT, and laboratory data retain a prognostic value even in patients who are not candidates for surgery regardless of the subsequent therapeutical option (TARE vs. systemic treatment).

Despite the observation that an important discordance between the two imaging methods in the assessment of lymph node involvement with $[^{18}\text{F}]$ -FDG-PET/CT showing a lower detection rate as compared to ceCT, an important correlation of PET N+ results with OS was found. This is probably due to the fact that the disease metabolic rate detected through the FDG uptake significantly impacts prognosis, while metastatic lymph nodes with a low metabolic rate (and consequently no FDG uptake) retain a lower prognostic meaning.

The main limitations of our study were the relatively low number of enrolled patients and the heterogeneity of pre-enrollment care. As patients with iCCA potentially candidate to TARE is not a common clinical condition, the therapeutical approach is not standardized yet (36). In our experience,

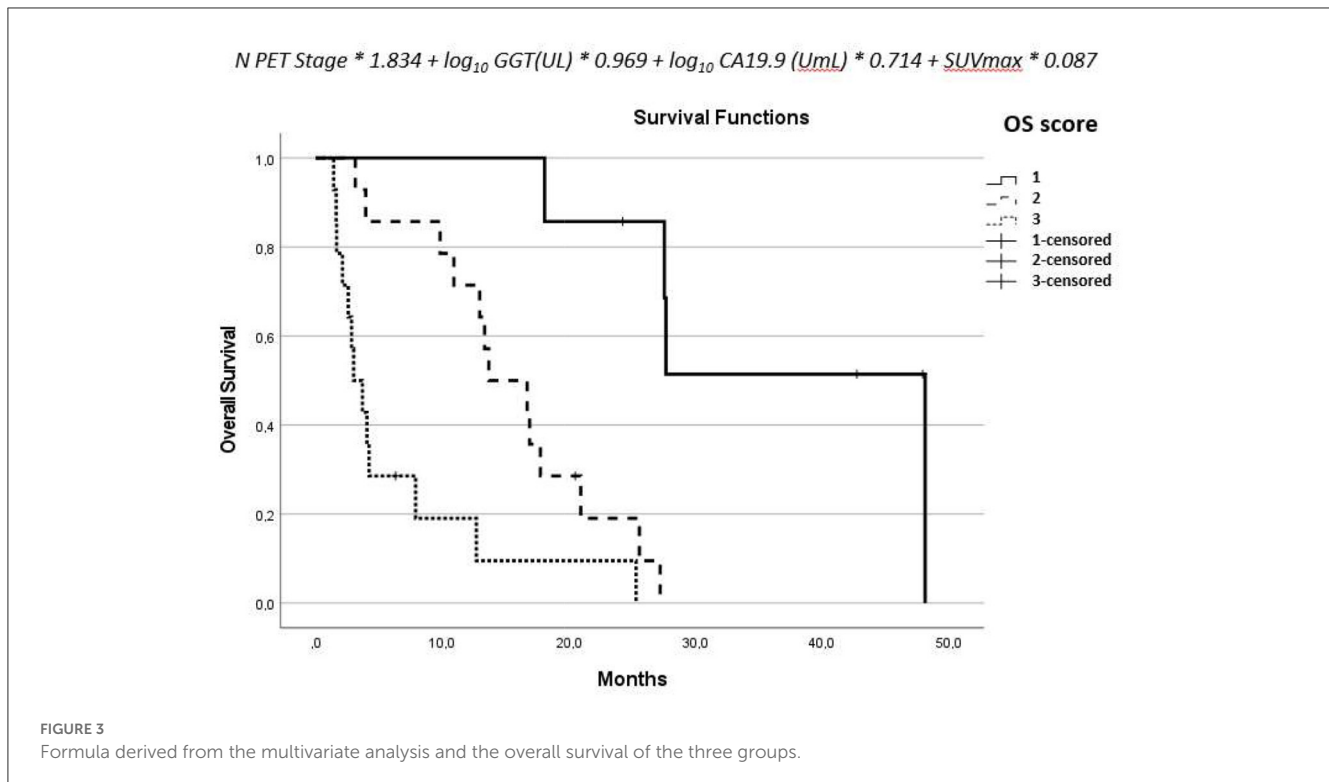
$[^{18}\text{F}]$ -FDG-PET/CT has proven to be crucial both for correctly assessing the extent of intra and extrahepatic disease significantly impacting subsequent treatment choice when associated with multiphase ceCT. This is witnessed by the relatively high number of patients who came to our center for TARE and were not treated after the imaging evaluation. This suggests that the routine use of $[^{18}\text{F}]$ -FDG-PET/CT and ceCT in clinical practice may have a significant impact on the therapeutic management of patients with iCCA and could potentially be proposed as a new imaging standard for the evaluation of TARE candidate patients.

Considering that, in addition to the parameters derived from multimodality imaging, laboratory data also showed a significant correlation with patient prognosis: we believe that the nomogram that we elaborated, combining $[^{18}\text{F}]$ -FDG-PET/CT, ceCT, and laboratory data, can be considered a useful tool for prognostic stratification.

5. Conclusion

Considering our data, performing integrated multimodality imaging is critical for the prognostic stratification of patients with iCCA.

Indeed, in our experience, while ceCT remains the reference imaging method in the staging of local disease, $[^{18}\text{F}]$ -FDG-PET/CT



has proven to be crucial in the lymph node and distant disease evaluation. In addition, semi-quantitative parameters, such as SUVmax, MTV, and TLG were also effective in the prognostic stratification of patients.

Data availability statement

The raw data supporting the conclusions of this article will be made available by the authors, without undue reservation.

Ethics statement

The studies involving human participants were reviewed and approved by Review Board and Ethical Committee of S. Orsola Hospital (193/2021/Oss/AOUBo). The patients/participants provided their written informed consent to participate in this study.

Author contributions

CN and CM: conceptualization and investigation. APac: methodology and formal analysis. VD and MB: data curation.

CN, CM, and MC: manuscript writing. SB and NE, and APal: manuscript writing-review and editing. GB and SF: supervision. All authors have read and agreed to the published version of the manuscript.

Conflict of interest

The authors declare that the research was conducted in the absence of any commercial or financial relationships that could be construed as a potential conflict of interest.

Publisher's note

All claims expressed in this article are solely those of the authors and do not necessarily represent those of their affiliated organizations, or those of the publisher, the editors and the reviewers. Any product that may be evaluated in this article, or claim that may be made by its manufacturer, is not guaranteed or endorsed by the publisher.

References

1. Welzel TM, McGlynn KA, Hsing AW, O'Brien TR, Pfeiffer RM. Impact of classification of hilar cholangiocarcinomas (Klatskin tumors) on the incidence of intra- and extrahepatic cholangiocarcinoma in the United States. *J Natl Cancer Inst.* (2006) 98:873–5. doi: 10.1093/jnci/djj234
2. Rizvi S, Gores GJ. Pathogenesis, diagnosis, and management of cholangiocarcinoma. *Gastroenterology.* (2013) 145:1215–29. doi: 10.1053/j.gastro.2013.10.013

3. Bergquist A, von Seth E. Epidemiology of cholangiocarcinoma. *Best Pract Res Clin Gastroenterol.* (2015) 29:221–32. doi: 10.1016/j.bpg.2015.02.003
4. Blechacz B, Komuta M, Roskams T, Gores GJ. Clinical diagnosis and staging of cholangiocarcinoma. *Nat Rev Gastroenterol Hepatol.* (2011) 8:512–22. doi: 10.1038/nrgastro.2011.131
5. Shaib Y, El-Serag HB. The epidemiology of cholangiocarcinoma. *Semin Liver Dis.* (2004) 24:115–25. doi: 10.1055/s-2004-828889
6. Shaib YH, Davila JA, McGlynn K, El-Serag HB. Rising incidence of intrahepatic cholangiocarcinoma in the United States: a true increase? *J Hepatol.* (2004) 40:472–7. doi: 10.1016/j.jhep.2003.11.030
7. Khan SA, Toledano MB, Taylor-Robinson SD. Epidemiology, risk factors, and pathogenesis of cholangiocarcinoma. *HPB.* (2008) 10:77–82. doi: 10.1080/13651820801992641
8. Blechacz BR, Gores GJ. Cholangiocarcinoma. *Clin Liver Dis.* (2008) 12:131–50. doi: 10.1016/j.cld.2007.11.003
9. Weber SM, Ribero D, O'Reilly EM, Kokudo N, Miyazaki M, Pawlik TM. Intrahepatic cholangiocarcinoma: expert consensus statement. *HPB.* (2015) 17:669–80. doi: 10.1111/hpb.12441
10. Spolverato G, Vitale A, Cucchetti A, Popescu I, Marques HP, Aldrighetti L, et al. Can hepatic resection provide a long-term cure for patients with intrahepatic cholangiocarcinoma? *Cancer.* (2015) 121:3998–4006. doi: 10.1002/cncr.29619
11. Petrowsky H, Wildbrett P, Husarik DB, Hany TF, Tam S, Jochum W, et al. Impact of integrated positron emission tomography and computed tomography on staging and management of gallbladder cancer and cholangiocarcinoma. *J Hepatol.* (2006) 45:43–50. doi: 10.1016/j.jhep.2006.03.009
12. Tsunematsu S, Chuma M, Kamiyama T, Miyamoto N, Yabusaki S, Hatanaka K, et al. Intratumoral artery on contrast-enhanced computed tomography imaging: differentiating intrahepatic cholangiocarcinoma from poorly differentiated hepatocellular carcinoma. *Abdom Imaging.* (2015) 40:1492–9. doi: 10.1007/s00261-015-0352-9
13. Zhang Y, Uchida M, Abe T, Nishimura H, Hayabuchi N, Nakashima Y. Intrahepatic peripheral cholangiocarcinoma: comparison of dynamic CT and dynamic MRI. *J Comput Assist Tomogr.* (1999) 23:670–7. doi: 10.1097/00004728-199909000-00004
14. Vilgrain V. Staging cholangiocarcinoma by imaging studies. *HPB.* (2008) 10:106–9. doi: 10.1080/13651820801992617
15. Okami J, Dono K, Sakon M, Tsujie M, Hayashi N, Fujiwara Y, et al. Patterns of regional lymph node involvement in intrahepatic cholangiocarcinoma of the left lobe. *J Gastrointest Surg.* (2003) 7:850–6. doi: 10.1007/s11605-003-0029-5
16. Baheti AD, Tirumani SH, Shinagare AB, Rosenthal MH, Hornick JL, Ramaiya NH, et al. Correlation of CT patterns of primary intrahepatic cholangiocarcinoma at the time of presentation with the metastatic spread and clinical outcomes: retrospective study of 92 patients. *Abdom Imaging.* (2014) 39:1193–201. doi: 10.1007/s00261-014-0167-0
17. You MW, Yun SJ. Differentiating between hepatocellular carcinoma and intrahepatic cholangiocarcinoma using contrast-enhanced MRI features: a systematic review and meta-analysis. *Clin Radiol.* (2019) 74:406. doi: 10.1016/j.crad.2018.12.016
18. Annunziata S, Caldarella C, Pizzuto DA, Galiano F, Sadeghi R, Giovannella L, et al. Diagnostic accuracy of fluorine-18-fluorodeoxyglucose positron emission tomography in the evaluation of the primary tumor in patients with cholangiocarcinoma: a meta-analysis. *Biomed Res Int.* (2014) 2014:247693. doi: 10.1155/2014/247693
19. Corvera CU, Blumgart LH, Akhurst T, DeMatteo RP, D'Angelica M, Fong Y, et al. 18F-fluorodeoxyglucose positron emission tomography influences management decisions in patients with biliary cancer. *J Am Coll Surg.* (2008) 206:57–65. doi: 10.1016/j.jamcollsurg.2007.07.002
20. Moon CM, Bang S, Chung JB, Park SW, Song SY, Yun M, et al. Usefulness of 18F-fluorodeoxyglucose positron emission tomography in differential diagnosis and staging of cholangiocarcinomas. *J Gastroenterol Hepatol.* (2008) 23:759–65. doi: 10.1111/j.1440-1746.2007.05173.x
21. Ma KW, Cheung TT, She WH, Chok KSH, Chan ACY, Dai WC, Chiu WH, et al. Diagnostic and prognostic role of 18-FDG PET/CT in the management of resectable biliary tract cancer. *World J Surg.* (2018) 42:823–34. doi: 10.1007/s00268-017-4192-3
22. Ikeno Y, Seo S, Iwasako K, Yoh T, Nakamoto Y, Fuji H, et al. Preoperative metabolic tumor volume of intrahepatic cholangiocarcinoma measured by 18F-FDG-PET is associated with the KRAS mutation status and prognosis. *J Transl Med.* (2018) 16:95. doi: 10.1186/s12967-018-1475-x
23. Boellaard R, Delgado-Bolton R, Oyen WJ, Giammarile F, Tatsch K, Eschner W, et al. FDG PET/CT: EANM procedure guidelines for tumour imaging: version 20. *Eur J Nucl Med Mol Imaging.* (2015) 42:328–54. doi: 10.1007/s00259-014-2961-x
24. Iatrou M, Ross SG, Manjeshwar RM, Stearns CW. A fully 3D iterative image reconstruction algorithm incorporating data corrections. *IEEE Symposium Conf. Rec. Nucl. Sci.* (2004) 4:2493–7. doi: 10.1109/NSSMIC.2004.1462761
25. Mosconi C, Gramenzi A, Ascanio S, Cappelli A, Renzulli M, Pettinato C, et al. Yttrium-90 radioembolization for unresectable/recurrent intrahepatic cholangiocarcinoma: a survival, efficacy and safety study. *Br J Cancer.* (2016) 115:297–302. doi: 10.1038/bjc.2016.191
26. Gramenzi A, Golfieri R, Mosconi C, Cappelli A, Granito A, Cucchetti A, et al. Yttrium-90 radioembolization vs sorafenib for intermediate-locally advanced hepatocellular carcinoma: a cohort study with propensity score analysis. *Liver Int.* (2015) 35:1036–47. doi: 10.1111/liv.12574
27. Fujita N, Asayama Y, Nishie A, Ishigami K, Ushijima Y, Takayama Y, et al. Mass-forming intrahepatic cholangiocarcinoma: enhancement patterns in the arterial phase of dynamic hepatic CT - correlation with clinicopathological findings. *Eur Radiol.* (2017) 27:498–506. doi: 10.1007/s00330-016-4386-3
28. Hewitt DB, Brown ZJ, Pawlik TM. Surgical management of intrahepatic cholangiocarcinoma. *Expert Rev Anticancer Ther.* (2022) 22:27–38. doi: 10.1080/14737140.2022.1999809
29. Panettieri E, Maki H, Kim BJ, Kang HC, Cox V, Vega EA, et al. Arterial enhancement pattern predicts survival in patients with resectable and unresectable intrahepatic cholangiocarcinoma. *Surg Oncol.* (2022) 40:101696. doi: 10.1016/j.suronc.2021.101696
30. Park HM, Jang HY, Lee DE, Kang MJ, Han SS, et al. Prognostic impact of tumor vascularity on CT in resectable intrahepatic cholangiocarcinoma. *HPB.* (2022) 24:359–69. doi: 10.1016/j.hpb.2021.06.424
31. Jolissaint JS, Wang T, Soares KC, Chou JF, Gönen M, Pak LM, et al. Machine learning radiomics can predict early liver recurrence after resection of intrahepatic cholangiocarcinoma. *HPB.* (2022) 24:1341–50. doi: 10.1016/j.hpb.2022.02.004
32. Mosconi C, Cucchetti A, Bruno A, Cappelli A, Bargellini I, De Benedittis C, et al. Radiomics of cholangiocarcinoma on pretreatment CT can identify patients who would best respond to radioembolisation. *Eur Radiol.* (2020) 30:4534–44. doi: 10.1007/s00330-020-06795-9
33. Kluge R, Schmidt F, Caca K, Barthel H, Hesse S, Georgi P, et al. Positron emission tomography with [(18)F]fluoro-2-deoxy-D-glucose for diagnosis and staging of bile duct cancer. *Hepatology.* (2001) 33:1029–35. doi: 10.1053/jhep.2001.23912
34. Kato T, Tsukamoto E, Kuge Y, Katoh C, Nambu T, Nobuta A, et al. Clinical role of (18)F-FDG PET for initial staging of patients with extrahepatic bile duct cancer. *Eur J Nucl Med Mol Imaging.* (2002) 29:1047–54. doi: 10.1007/s00259-002-0852-z
35. Fritscher-Ravens A, Bohuslavizki KH, Broering DC, Jenicke L, Schäfer H, Buchert R, et al. in the diagnosis of hilar cholangiocarcinoma. *Nucl Med Commun.* (2001) 22:1277–85. doi: 10.1097/00006231-200112000-00002
36. Valle JW, Borbath I, Khan SA, Huguet F, Gruenberger T, Arnold D. ESMO Guidelines Committee. Biliary cancer: ESMO clinical practice guidelines for diagnosis, treatment and follow-up. *Ann Oncol.* (2016) 27:v28–37. doi: 10.1093/annonc/mdw324